Laser and Particle Beams (2009), *27*, 643–649.

doi:10.1017/S0263034609990486

Experimental investigation of fast electron transport in solid density matter: Recent results from a new technique of X-ray energy-encoded 2D imaging

L. LABATE,[1,2,3] E. FÖRSTER,[4] A. GIULIETTI,[1,2] D. GIULIETTI,[2,3,5] S. HÖFER,[4] T. KÄMPFER,[4] P. KÖSTER,[1,2] M. KOZLOVA,[6] T. LEVATO,[1,3] R. LÖTZSCH,[4] A. LÜBCKE,[4] T. MOCEK,[6] J. POLAN,[6] B. RUS,[6] I. USCHMANN,[4] F. ZAMPONI,[4] AND L.A. GIZZI[1,2,3]

[1]Intense Laser Irradiation Laboratory, IPCF, Consiglio Nazionale delle Ricerche, Pisa, Italy
[2]Istituto Nazionale di Fisica Nucleare, Sezione di Pisa, Italy
[3]Laboratori Nazionali di Frascati, Istituto Nazionale di Fisica Nucleare, Frascati, Italy
[4]Institut für Optik und Quantenelektronik, Friedrich-Schiller-Universität, Jena, Germany
[5]Dipartimento di Fisica, Universitá di Pisa, Italy
[6]Department of X-ray Lasers, PALS Centre-Institute of Physics, Prague, Czech Republic

(Received 2 May 2009; Accepted 31 August 2009)

Abstract

The development activity of a new experimental technique for the study of the fast electron transport in high density matter is reported. This new diagnostic tool enables the X-ray 2D imaging of ultrahigh intensity laser plasmas with simultaneous spectral resolution in a very large energy range to be obtained. Results from recent experiments are discussed, in which the electron propagation in multilayer targets was studied by using the Kα. In particular, results highlighting the role of anisotropic Bremsstrahlung are reported, for the sake of the explanation of the capabilities of the new diagnostics. A discussion of a test experiment conceived to extend the technique to a single-shot operation is finally given.

Keywords: Anisotropic Bremsstrahlung; Fast electron diagnostics; Fast electron transport; High-density matter; Relativistic electrons

1. INTRODUCTION

The issue of fast electron transport in high-density matter is currently receiving growing attention, both from a theoretical (Bret & Deutsch, 2006; Deutsch *et al.*, 2008*a*, 2008*b*; Evans, 2006; Honrubia *et al.*, 2006, 2004) and an experimental viewpoint (Batani, 2002; Nakamura *et al.*, 2006), even in view of its crucial role in the *fast ignitor* approach to the inertial confinement fusion (ICF) (Atzeni, 1999; Kodama *et al.*, 2001; Sakagami *et al.*, 2006; Sherlock *et al.*, 2006; Tabak *et al.*, 1994). Indeed, as it is well known, within this scheme, the ignition of a small *hot spot*, having linear dimensions on the order of 10 μm, in the pre-compressed DT fuel is expected to be reached by means of the energy deposition by a high-current (well beyond the Alfvèn limit) beam of relativistic electrons, with kinetic energy $E_k \gtrsim 1$ MeV (Tabak *et al.*, 2005). As it came out during the last few years, the propagation of such a high current beam, which would ideally have to occur through the compressed, high-density plasma, cannot be described by simple collisional, "Bethe-Bloch like" models. Indeed, the role played by the self-generated electric and magnetic fields cannot be neglected (Batani, 2002; Bell *et al.*, 1997; Davies, 2004). As it is known, this leads, as an example, to the need of a return current in order for the propagation to occur over the required distances, as well as to self-pinching effects of the electron beam. Moreover, the instabilities of the fast electron beam in the presence of the cold electron return current, such as e.g., the filamentation instability (Gremillet *et al.*, 2002), should be considered.

From an experimental point of view, the investigation of the fast electron transport in high density matter is mostly performed by irradiating solid targets. In this field, the main diagnostics is the *K*α emission spectroscopy, eventually from *ad hoc* fluorescent tracer layers, which is routinely performed by using bent (spherical or toroidal) Bragg crystals coupled either to X-ray film (or image plates) or to charge

Address correspondence and reprint requests to: L. Labate, Intense Laser Irradiation Laboratory, IPCF, Consiglio Nazionale delle Ricerche, Pisa, Italy. E-mail: luca.labate@ipcf.cnr.it

coupled device (CCD) cameras (Baton *et al.*, 2008; Köster *et al.*, 2009; Labate *et al.*, 2004, 2007*a*; Lancaster *et al.*, 2007). Bent crystals allow the spectrum and a one-dimensional (1D) image of an X-ray source to be simultaneously obtained, with resolving power $\lambda/\Delta\lambda \sim 10^3$ and spatial resolution down to a few μm, mainly dependent on the detector used (Faenov *et al.*, 2008; Labate *et al.*, 2005; Nishimura *et al.*, 2003; Young *et al.*, 1998). As an alternative, two-dimensional (2D) images of the source, with the same figure for the spatial resolution, can be obtained at a fixed photon wavelength.

While allowing a very high spectral resolution to be obtained, bent Bragg crystals suffer from a low diffraction efficiency (Missalla *et al.*, 1999). Moreover, a fundamental issue about the ultimate signal-to-noise (S/N) ratio comes from the fluorescence and Compton radiation produced by the crystal when exposed to hard X-rays, as well as to X-ray radiation due to the interaction of high energy particles with the crystal itself. It is clear that this issue deserves careful consideration in the case of ultrahigh intensity laser-plasma interaction experiments related to ICF.

A basic feature of bent crystals is the small spectral range available for a given configuration (i.e., in a given shot). This is of course related to their high dispersing power and to the high spectral resolution achievable. However, this can be an important limitation when, e.g., the $K\alpha$ emission from both cold and ionized particles has to be simultaneously observed (King *et al.*, 2005). For the same reason, Bremsstrahlung continuum radiation is also very difficult to study using Bragg crystals. Furthermore, this demands for the use of different crystals for different tracer layers, i.e., different elements. It is worthwile to cite at this point that a new concept diagnostics has been recently developed, consisting of a flat Bragg crystal coupled to a pinhole array. Monochromatic X-ray images of an ICF target at different X-ray wavelength in a narrow range from about 3.5 to 4.1 keV have been simultaneously recorded in this way (Tommasini *et al.*, 2006).

All of the above issues must be taken into account in the design of experiments devoted to the investigation of fast electron transport in ICF relevant conditions. Indeed, the development of new kinds of diagnostics is an important aspect for the projects pursuing the fast ignition approach, such as the HiPER project (HiPER project, 2008). We observe here that recent advances have been reported in the field of the diagnostic tools for the mixed space and time-resolved investigation of the X-ray emission from plasmas in ICF relevant conditions, based upon new concept streak-camera devices (Huang *et al.*, 2006; Zhong *et al.*, 2008).

In this paper, we report on the results of some recent experiments devoted to the development of a new experimental technique for the X-ray imaging of laser plasmas. The technique is based upon the use of a CCD detector operating in the single-photon regime, coupled to a pinhole. As it is well known, CCD detectors allow, when operating in the single-photon regime, the X-ray spectrum of the impinging radiation to be retrieved, without any external energy dispersing device, basically due to the linear relationship between the X-ray photon energy and the released (and collected) charge (Labate *et al.*, 2008; Levato *et al.*, 2008; Zamponi *et al.*, 2005). CCD detectors in such a configuration have been used for a long time in laser-plasma experiments to get an X/γ-ray spectrum over a broad range (Beg *et al.*, 1997; Gizzi *et al.*, 1996; Key *et al.*, 2008; Stoeckl *et al.*, 2004). If a pinhole is inserted between the source and the detector, each detected X-ray photon, whose energy can be retrieved according to the above considerations, also keeps an encoded 2D spatial information on its origin (or, *vice-versa*, one can think to a 2Dimage with an encoded energy information), so that one has a sort of single-photon pinhole camera. By collecting a sufficient number of photons, it is thus possible to get simultaneously the 2D images of the source at any photon energy in the sensitive range of the CCD detector (Levato *et al.*, 2008), provided that a sufficient number of photons in the desired energy bin has been collected.

From a practical point of view, this can be accomplished either by relying on a large number of acquisitions (that is, laser shots) in the same experimental conditions or by using a large number of pinholes (in other words, using a large number of "single-photon pinhole cameras" at the same time, each of them using a different region of the same CCD detector). Only the second approach is applicable on a single-shot basis and can be used at low-repetition rate laser facilities. In what follows, we give an outline of some recent experiments carried out by our group using the first approach (that is, using the technique on a multi-shot basis) and then we briefly show some results from an *ad hoc* experiment devoted to extend our technique to single-shot operation.

2. THE TYPICAL EXPERIMENTAL SETUP AND A BRIEF DESCRIPTION OF THE TECHNIQUE

The first experiment using our new technique of X-ray energy-encoded 2D imaging was carried out at the IOQ-Jena facility with the "JeTi" Ti:sapphire laser system, providing 70 fs duration pulses with an energy of 600 mJ at a repetition rate of 10 Hz.

Figure 1 shows a sketch of the typical experimental setup inside the vacuum chamber. The laser pulse was focused onto the surface of solid targets by means of a 45°, $f/1.2$ off-axis parabola (OAP), at an angle incidence of about 10°. The spot size was about 5 μm^2 and the maximum intensity about 5×10^{19} W/cm^2 ($a_0 = eA_L/m_ec^2 \simeq 4.8$). The figure shows two identical single-photon pinhole cameras, looking at the target from different directions. Each pinhole camera consisted of a 5 μm diameter pinhole coupled to a back-illuminated, cooled X-ray CCD camera. In this particular experiment, each pinhole was bored in a 25 μm thick Pt substrate. Two deep-depletion Andor DX420 CCD cameras were used, whose chips were cooled

https://doi.org/10.1017/S0263034609990486 Published online by Cambridge University Press

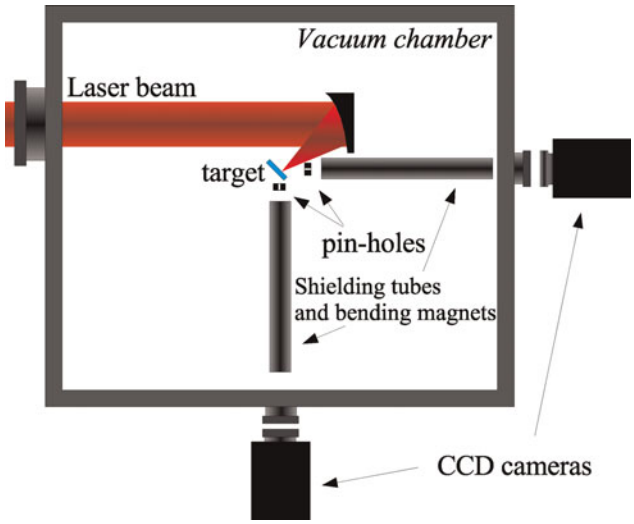

Fig. 1. (Color online) Sketch of the typical experimental setup used in our experiments.

down to -65°C in order to reduce the thermal noise due to the dark current. The pixel size for such a CCD model is $26 \times 26\ \mu m^2$ and the magnification of our pinhole cameras was $M \simeq 10$. These values lead to an estimate for the ultimate spatial resolution of about 5 μm, limited by the pinhole size. In the experiment of Figure 1, due to the vacuum chamber size, the CCD cameras were put outside of the main chamber, each of them in its own separate small vacuum chamber, and 50 μm thick *kapton* foils were used as X-ray transparent windows.

As it is visible in the figure, the whole path from the pinhole to the CCD (actually, in this case, to the vacuum flange) was shielded by 1 cm thick lead tubes. Moreover, inside these tubes, along their whole length, a set of small magnets was put, producing an estimated field of about 0.3 T at the tube center, in order to prevent high-energy charged particles from reaching the CCD chip or the filters in front of it. The CCD body was also shielded by some millimeters thick lead. These kinds of shielding are of crucial importance when the CCD has to be operated in the single-photon regime, in particular in ultrahigh intensity experiments (Stoeckl *et al.*, 2004).

The details of the technique and the data analysis can be found in Labate *et al.* (2007*b*). We only mention here that the CCD is forced to operate in the single-photon regime by using a large number of thin mylar foils in front of it. In the case of the experiment to which Figure 1 refers (that is, with an X-ray source size of about 10 μm, a magnification factor $M \simeq 10$, and a pixel size $26 \times 26\ \mu m^2$), a few tens of photons per shot were detected. By summing up the "single-photon images" of about 350 laser shots (after a center-of-mass retrieving algorithm correction taking care of the possible target displacement from shot to shot (Labate *et al.*, 2007*b*)) an energy-encoded 2D image of the X-ray source was obtained, having a spatial resolution of 5 μm and a spectral resolution of about 150 eV, typical of single-photon CCD spectrometers (Bootsma *et al.*, 2000). In other words, beside the X-ray spectrum in a range extending over a few tens of keV (that is, over the detector useful range), 2D images are reconstructed at any photon energy within this range, integrated over an energy interval comparable to the energy resolution. We will show in the next section some experimental results.

3. APPLICATION TO THE STUDY OF FAST ELECTRON TRANSPORT AND X-RAY EMISSION IN MULTILAYER TARGETS

As anticipated in the introduction, the most direct way of studying the propagation of high-current electron beams in high-density matter is the Kα spectroscopy with spatial resolution (Freeman *et al.*, 2003; Nishimura *et al.*, 2003). In such a context, a major, standard class of experiments makes use of Kα fluorescent multilayer targets, whose Kα emission from the different tracer layers allows the propagation of the fast electrons to be followed at different depths inside the target. It is worthwile observing at this point that the study of the Kα emission from thin solid targets also deserves its own interest in view of the optimization of Kα based ultrashort, and ultraintense X-ray sources for applications. In this section, we show some results obtained using our new imaging technique, aiming to illustrate how it can be employed in the context of fast electron transport studies.

Figure 2 (left) shows the X-ray spectrum in the 4–10 keV range from a three layer target (Ti-mylar-Cu) irradiated with the laser pulse whose parameters have been given in Section 2. The spectrum was retrieved by using our technique after 350 laser shots. Figure 2 (right) shows instead the 2D image of the emitting source at the Ti and Cu Kα/β energy; in other words, the upper (lower) image is obtained by summing up the contributions from only those photons at the Ti (Cu) Kα or Kβ energy. We notice here that our technique is not limited to image out the source only at selected photon energies corresponding to emission lines. In principle, an image of the X-ray source can be retrieved at any wavelength range, provided a sufficient number of photons has been collected in that range. It is thus clear that the Bremsstrahlung emission can be studied in this way and the corresponding absolute photon flux can be retrieved. This is an important feature of the technique, even in view of the fact that the Bremsstrahlung emission is related to the fast electron beam transport (Chen *et al.*, 2001; Norreys *et al.*, 1999; Sentoku *et al.*, 1998).

In order to highlight the role of the Bremsstrahlung emission on our X-ray measurements, we observe that we found in most of our experiments a systematic difference between the sizes of the same source (that is, the source at a given energy) as seen from the front and from the back side of the target (even after a correction for eventual different viewing angles). Our observations suggest an underlying non-isotropic emission process involved. As an example, we consider the simple case of a one layer Ti thin target.

https://doi.org/10.1017/S0263034609990486 Published online by Cambridge University Press

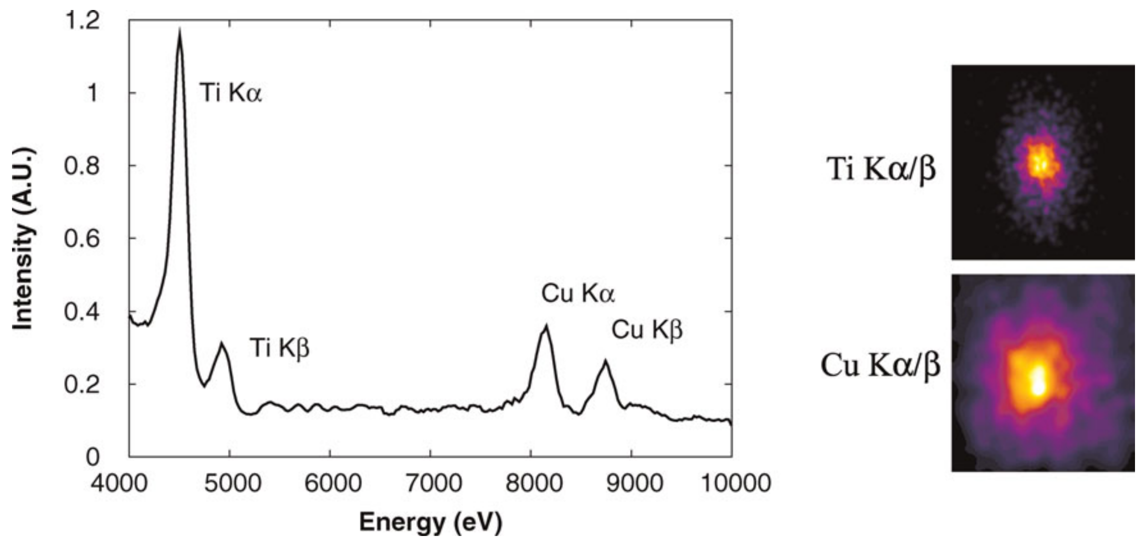

Fig. 2. (Color online) X-ray spectrum (**left**) and energy resolved X-ray images at two different photon energies (**right**) of a Ti-mylar-Cu multi-layer target irradiated at an intensity of 5×10^{19} W/cm^2, as obtained with the diagnostics discussed in the text from 350 laser shots. The two images on the right both have a size of 200×200 μm (on the object plane) and are not comparable to each other as for the color scale.

The X-ray source at the Ti Kα energy as seen from the back side of the target appeared to be larger (by a factor $\sim 2-3$, for foil thicknesses between 5 and 25 μm) than the same source as seen from the front side.

A possible explanation for this difference comes from Figure 3, showing the emission spectrum around the Ti Kα line as seen from the front (a) and the back (b) side of the target. For each viewing direction, different spectra are reported, obtained considering photons coming from regions at different distances from the source center (defined as the point where the maximum of the emission occurs). The plots clearly show that a continuum spectral component contributes to the observed emission at the Kα energy on the front side (Fig. 3a). Furthermore, this component comes from a small region around the source center. Based upon previously published literature (Li *et al.*, 2006; Sentoku *et al.*, 1998; Sheng *et al.*, 2000), this emission has been attributed to directional electron Bremsstrahlung occurring on the front side of the target (Zamponi *et al.*, 2009).

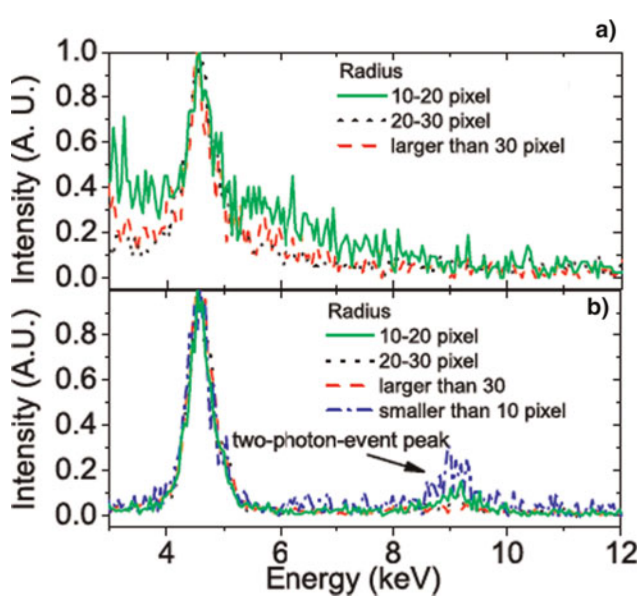

Fig. 3. (Color online) X-ray spectrum of a 5 μm thick Ti foil irradiated at an intensity of 5×10^{19} W/cm^2, as observed from the front (**a**) and from the back (**b**) side of the target (both at an angle of 45° with respect to the target surface). For each case, the spectra reconstructed by adding up the contributions from photons coming from different anular regions of the source are shown. The different regions are identified by the distance (radius) from the source center (defined as the point where the maximum of the X-ray emission occurs). The pixel size was 26×26 μm^2 and the magnification was $M \simeq 10$.

4. A TEST EXPERIMENT TOWARD A SINGLE-SHOT ENERGY-ENCODED 2D IMAGING

Due to the requirement for the single-photon condition to be fulfilled and to the need for a sufficient photon statistics, the diagnostic approach as described above requires a large number of laser shots. Its use in ICF relevant experiments at low repetition rate facilities thus requires an *ad hoc* extension to a single-shot operation. A possibility toward this goal is offered by the recent large area CCD detectors, which allow a large number of "single-photon images," separated in space on the detector plane, to be acquired. In other words, an array of closely spaced pinholes is used instead of a single pinhole. The resulting data can then be brought back to the case of a single pinhole once the position on the CCD detector of the centers of the images relative to the different pinholes are known.

Fig. 4. (Color online) (**left**) SEM image of a pinhole array made from a 100 μm thick W substrate. A close view of a single pinhole is also shown. (**right**) Energy resolved X-ray image at the Ti Kα/β photon energy of a Ti thick target irradiated at an intensity of about 2×10^{14} W/cm^2. The image has a size of 60×60 μm in the object plane.

A technique for the production of the pinhole array has been recently developed at our laboratory, which allowed us to make a pinhole array by tightly focusing the frequency doubled beam of a TiSa 0.2 TW laser system onto a 100 μm thick W foil. Figure 4 shows a SEM image of the pinhole array, showing very good shaped nearly cilindrical holes with a diameter of about 5–7 μm. The array holds a total of 20×20 pinholes on a nearly rectangular grid with 60 μm spacing. A test experiment has been carried out at the PALS laboratory in Prague, where the 3rd harmonic of the PALS iodine laser ($\lambda \simeq 0.438$ μm) has been focused on a thick Ti target at an intensity of about 2×10^{14} W/cm^2. Figure 4 (right) shows, as an example, the image of the X-ray source at the Ti Kα/β photon energy as obtained with our technique from a singe shot, showing a source size of about 30 μm. It should be noted here that, when the source size d_s is not considerably smaller than the pinhole distance d_{ph}, an overlapping between the images coming from neighboring pinholes may actually affect the retrieved image. Due to this issue, the image size of the shown figure is actually the largest that one could get with the pinhole array shown. This issue can be clearly addressed by using a larger spacing pinhole array. Thus, the validity of the condition $d_s \ll d_{ph}$ should be preliminarly assessed in order to safely employing such a diagnostic technique. In other words, the choice of the pinhole distance has to be carefully chosen using a preliminary, rough estimate of the source size.

5. SUMMARY AND CONCLUSIONS

The development of new experimental tools for the simultaneous X-ray imaging and spectroscopy of laser-matter interaction at ultrahigh intensity is an important issue in the field of the fast ignition. A new technique for the X-ray 2D imaging with simultaneous spectral resolution has been developed. The technique described here is based upon the scheme of a simple X-ray pinhole camera, which further exploits the CCD detector capability to provide the spectrum of the incoming radiation when operating in the single-photon regime. Some experiments devoted to the study of the fast electron transport in solid density matter have been successfully carried out, whose results have been reported here in order to illustrate the new technique.

The diagnostics is now being extended to single shot operation, by using an approach based upon a pinhole array coupled to a large area CCD detector. A test experiment has been carried out, which showed the feasibility of such an approach.

ACKNOWLEDGEMENTS

The Pisa authors wish to acknowledge support from the Italian MIUR projects FISR "Impianti innovativi multiscopo per la produzione di radiazione X ed ultravioletta," FIRB "BLISS – Broadband Laser for ICF Strategic Studies," and "SPARX" and PRIN "Studio della generazione e della propagazione di elettroni rapidi". The Pisa group also acknowledge support from the INFN project "PLASMONX" and the EU FP7 program "HiPER". We acknowledge support from the Deutsche Forshungsgemeinschaft for the financial support. The access to the Jena and to the Prague facilities was granted by the LASERLAB initiative of the EU FP6.

REFERENCES

Atzeni, S. (1999). Inertial fusion fast ignitor: Igniting pulse parameter window vs the penetration depth of the heating particles and the density of the precompressed fuel. *Phys. Plasmas* **6**, 3316–3326.

Batani, D. (2002). Transport in dense matter of relativistic electron produced in ultra-high-intensity laser interactions. *Laser Part. Beams* **20**, 321–336.

Baton, S.D., Koenig, M., Fuchs, J., Benuzzi-Mounaix, A., Guillou, P., Loupias, B., Vinci, T., Gremillet, L., Rousseaux, C., Drouin, M., Lefebvre, E., Dorchies, F., Fourment, C., Santos, J.J., Batani, D., Morace, A., Redaelli, R., Nakatsutsumi, M., Kodama, R., Nishida, A., Ozaki, N., Norimatsu, T., Aglitskiy, Y., Atzeni, S. & Schiavi, A. (2008). Inhibition of fast electron energy deposition due to preplasma filling of cone-attached targets. *Phys. Plasma* **15**, 042706.

Beg, F.N., Bell, A.R., Dangor, A.E., Danson, C.N., Dews, A.P., Glinsky, M.E., Hammel, B.A., Lee, P., Norreys, P.A. &

Tatarakis, M. (1997). A study of picosecond laser-solid interactions up to 10^{19} W/cm^{-2}. *Phys. Plasmas* **4**, 447–457.

Bell, A.R., Davies, J.R., Guerin, S. & Ruhl, H. (1997). Fast-electron transport in high-intensity short-pulse laser-solid experiments. *Plasma Phys. Contr. Fusion* **39**, 653–659.

Bootsma, T.M.V., van Zwet, E.J., Brinkman, A.G., den Herder, J.W., de Jong, L., de Korte, P. & Olsthoorn, S.M. (2000). Synchrotron calibration and response modelling of back-illuminated xmm-rgs ccds. *Nucl. Instr. Meth. Phys. Res. A* **439**, 575–581.

Bret, A. & Deutsch, C. (2006). Density gradient effects on beam plasma linear instabilities for fast ignition scenario. *Laser Part. Beams* **24**, 269–273.

Chen, L.M., Zhang, J., Li, Y.T., Teng, H., Liang, T.J., Sheng, S.M., Dong, Q.L., Zhao, L.Z., Wei, Z.Y. & Tang, X.W. (2001). Effects of laser polarization on jet emission of fast electrons in femtosecond-laser plasmas. *Phys. Rev. Lett*. **87**, 225001.

Davies, J.R. (2004). Alfvèn limit in fast ignition. *Phys. Rev. E* **69**, 065402.

Deutsch, C., Bret, A., Firpo, M.C., Gremillet, L., Lefebvre, E. & Lifschitz, A. (2008*a*). Onset of coherent electromagnetic structures in the relativistic electron beam deuterium-tritium fuel interaction of fast ignition concern. *Laser Part. Beams* **26**, 157–165.

Deutsch, C., Bret, A., Firpo, M.C., Gremillet, L., Lefebvre, E. & Lifschitz, A. (2008*b*). Onset of coherent electromagnetic structures in the relativistic electron beam deuterium-tritium fuel interaction of fast ignition concern. *Laser Part. Beams* **26**, 507–507.

Evans, R.G. (2006). Modelling short pulse, high intensity laser plasma interactions. *Hi. Ener. Density Phys*. **2**, 35–47.

Faenov, A.Y., Magunov, A.I., Pikuz, T.A., Skobelev, I.Y., Giulietti, D., Betti, S., Galimberti, M., Gamucci, A., Giulietti, A., Gizzi, L.A., Labate, L., Levato, T., Tomassini, P., Marques, J.R., Bourgeois, N., Dobosz Dufrenoy, S., Ceccotti, T., Monot, P., Reau, F., Popescu, H., D'Oliveira, P., Martin, P., Fukuda, Y., Boldarev, A.S., Gasilov, S.V. & Gasilov, V.A. (2008). Non-adiabatic cluster expansion after ultrashort laser interaction. *Laser Part. Beams* **26**, 69–82.

Freeman, R., Anderson, C., Hill, J.M., King, J., Snavely, R., Hatchett, S., Key, M., Koch, J., MacKinnon, A., Stephens, R. & Cowan, T. (2003). Understanding the role of fast electrons in the heating of dense matter: Experimental techniques and recent results. *J Quant. Spectr. Rad. Trans* **81**, 183–190.

Gizzi, L.A., Giulietti, A., Giulietti, D., Audebert, P., Bastiani, S., Geindre, J.P. & Mysyrowicz, A. (1996). Simultaneous measurements of hard X-rays and second-harmonic emission in fs laser-target interactions. *Phys. Rev. Lett*. **76**, 2278–2281.

Gremillet, L., Bonnaud, G. & Amiranoff, F. (2002). Filamented transport of laser-generated relativistic electrons penetrating a solid target. *Phys. Plasma* **9**, 941–948.

HiPER project (2008). http://www.hiper-laser.org.

Honrubia, J.J., Alfonsìn, C., Alonso, L., Pèrez, B. & Cerrada, J.A. (2006). Simulations of heating of solid targets by fast electrons. *Laser Part. Beams* **24**, 217–222.

Honrubia, J.J., Antonicci, A. & Moreno, D. (2004). Hybrid simulations of fast electron transport in conducting media. *Laser Part. Beams* **22**, 129–135.

Huang, T.X., Nakai, M., Shiraga, H., Azechi, H., Huang, T.X., Ding, Y.K. & Zheng, Z.J. (2006). Ultrafast X-ray imaging with sliced sampling streak cameras. *Rev. Sci. Instr*. **77**, 026105.

Key, M.H., Adam, J.C., Akli, K.U., Borghesi, M., Chen, M.H., Evans, R.G., Freeman, R.R., Habara, H., Hatchett, S.P., Hill, J.M., Heron, A., ad King, J.A., Kodama, R., Lancaster, K.L., MacKinnon, A.J., Patel, P., Phillips, T., Romagnani, L., Snavely, R.A., Stephens, R., Stoeckl, C., Townn, T., Toyama, Y., Zhang, B., Zepf, M. & Norreys, P.A. (2008). Fast ignition relevant study of the flux of high-intensity laser-generated electrons via a hollow cone into a laser-imploded plasma. *Phys. Plasmas* **15**, 022701.

King, J.A., Akli, K., Snavely, R.A., Zhang, B., Key, M.H., Chen, C.D., Chen, M., Hatchett, S.P., Koch, J.A., MacKinnon, A.J., Patel, P.K., Phillips, T., Town, R.P.J., Freeman, R.R., Borghesi, M., Romagnani, L., Zepf, M., Cowan, T., Stephens, R., Lancaster, K.L., Murphy, C.D., Norreys, P. & Stoeckl, C. (2005). Characterization of a picosecond laser generated 4.5 KeV Ti K-alpha source for pulsed radiography. *Rev. Sci. Instr*. **76**, 076102.

Kodama, R., Norreys, P.A., Mima, K., Dangor, A.E., Evans, R.G., Fujita, H., Kitagawa, Y., Krushelnick, K., Miyakoshi, T., Miyanaga, N., Norimatsu, T., Rose, S.J., Shozaki, T., Shigemori, K., Sunahara, A., Tampo, M., Tanaka, K.A., Toyama, Y., Yamanaka, T. & Zepf, M. (2001). Fast heating of ultrahigh-density plasma as a step towards laser fusion ignition. *Nat*. **412**, 798–802.

Köster, P., Akli, K., Batani, D., Baton, S., Evans, R.G., Giulietti, A., Giulietti, D., Gizzi, L.A., Green, J.S., Koenig, M., Labate, L., Morace, A., Norreys, P., Perez, F., Waugh, J., Woolsey, N. & Lancaster, K.L. (2009). Experimental investigation of fast electron transport through Kα imaging and spectroscopy in relativistic laser-solid interactions. *Plasma Phys. Contr. Fusion* **51**, 014007.

Labate, L., Cecchetti, C.A., Galimberti, M., Giulietti, A., Giulietti, D. & Gizzi, L.A. (2005). Detailed characterization of the early X-ray emission of a plasma produced by point-like laser irradiation of solid Al targets. *Phys. Plasma* **12**, 083101.

Labate, L., Galimberti, M., Giulietti, A., Giulietti, D., Gizzi, L.A., Köster, P., Laville, S. & Tomassini, P. (2004). Ray-tracing simulations of a bent crystal X-ray optics for imaging using laser-plasma X-ray sources. *Laser Part. Beams* **22**, 253–259.

Labate, L., Galimberti, M., Giulietti, A., Giulietti, D., Köster, P., Tomassini, P. & Gizzi, L.A. (2007*a*). Study of forward accelerated fast electrons in ultrashort Ti Kα sources. *Appl. Phys. B* **86**, 229–233.

Labate, L., Giulietti, A., Giulietti, D., Köster, P., Levato, T., Gizzi, L.A., Zamponi, F., Lübcke, A., Kämpfer, T., Uschmann, I. & Förster, E. (2007*b*). Novel X-ray multispectral imaging of ultraintense laser plasmas by a single-photon charge coupled device based pinhole camera. *Rev. Sci. Instr*. **78**, 103506.

Labate, L., Levato, T., Galimberti, M., Giulietti, A., Giulietti, D., Sanna, M., Traino, C., Lazzeri, M. & Gizzi, L.A. (2008). A single-photon ccd-based setup for in situ measurement of the X-ray spectrum of mammographic units. *Nucl. Instr. Meth. Phys. Res. A* **594**, 278–282.

Lancaster, K.L., Green, J.S., Hey, D.S., Akli, K.U., Davies, J.R., Clarke, R.J., Freeman, R.R., Habara, H., Key, M.H., Kodama, R., Krushelnick, K., Murphy, C.D., Nakatsutsumi, M., Simpson, P., Stephens, R., Stoeckl, C., Yabuuchi, T., Zepf, M. & Norreys, P.A. (2007). Measurements of energy transport patterns in solid density laser plasma interactions at intensities of 5×10^{20} W/cm^{-2}. *Phys. Rev. Lett*. **98**, 125002.

Levato, T., Labate, L., Galimberti, M., Giulietti, A., Giulietti, D. & Gizzi, L.A. (2008). Detailed analysis of events from high-energy X-ray photons impinging on a two-phase front-illuminated ccd. *Nucl. Instr. Meth. Phys. Res. A* **592**, 346–353.

Li, Y.T., Yuan, X.H., Xu, M.H., Zheng, Z.Y., Sheng, Z.M., Chen, M., Ma, Y.Y., Liang, W.X., Yu, Q.Z., Zhang, Y., Liu, F., Wang, Z.H., Wei, Z.Y., Zhao, W., Jin, Z. & Zhang, J. (2006). Observation of a fast electron beam emitted along the surface of a target irradiated by intense femtosecond laser pulses. *Phys. Rev. Lett*. **96**, 165003.

Missalla, T., Uschmann, I., Förster, E., Jenke, G. & von der Linde, D. (1999). Monochromatic focusing of subpicosecond X-ray pulses in the kev range. *Rev. Sci. Instr*. **70**, 1288–1299.

Nakamura, T., Sakagami, H., Johzaki, T., Nagatomo, H. & Mima, K. (2006). Generation and transport of fast electrons inside cone targets irradiated by intense laser pulses. *Laser Part. Beams* **24**, 5–8.

Nishimura, H., Kawamura, T., Matsui, R., Ochi, Y., Okihara, S., Sakabe, S., Koike, F., Johzaki, T., Nagatomo, H., Mima, K., Uschmann, I. & Förster, E. (2003). Kα spectroscopy to study energy transport in ultrahigh-intensity laser produced plasmas. *J. Quan. Spectr. Rad. Trans*. **81**, 327–337.

Norreys, P.A., Santala, M., Clark, E., Zepf, M., Watts, F., Beg, F.N., Krushelnick, K., Tatarakis, M., Dangor, A.E., Fang, X., Graham, P., McCanny, T., Singhal, R.P., Ledingham, K.W.D., Creswell, A., Sanderson, D.C.W., Magill, J., Machacek, A., Wark, J., Allott, R., Kennedy, B. & Neely, D. (1999). Observation of a highly directional γ-ray beam from ultrashort, ultraintense laser pulse interactions with solids. *Phys. Plasma* **6**, 2150–2156.

Sakagami, H., Johzaki, T., Nagatomo, H. & Mima, K. (2006). Fast ignition integrated interconnecting code project for cone-guided targets. *Laser Part. Beams* **24**, 191–198.

Sentoku, Y., Mima, K., Taguchi, T., Miyamoto, S. & Kishimoto, Y. (1998). Particle simulation on X-ray emissions from ultra-intense laser produced plasmas. *Phys. Plasma* **5**, 4366–4372.

Sheng, Z.M., Sentoku, Y., Mima, K., Zhang, J., Yu, W. & Meyer-ter Vehn, J. (2000). Angular distributions of fast electron, ions, and bremsstrahlung X/γ-rays in intense laser interaction with solid targets. *Physi. Revi. Lett.* **85**, 5340–5343.

Sherlock, M., Bell, A.R. & Rozmus, W. (2006). Absorption of ultra-short laser pulses and particle transport in dense targets. *Laser Part. Beams* **24**, 231–234.

Stoeckl, C., Theobald, W., Sangster, T.C., Key, M.H., Patel, P., Zhang, B.B., Clarke, R., Karsch, S. & Norreys, P. (2004). Operation of a single-photon-counting X-ray charge-coupled device camera spectrometer in a petawatt environment. *Rev. Sci. Instr*. **75**, 3705–3707.

Tabak, M., Clark, D.S., Hatchett, S.P., Key, M.H., Lasinski, B.F., Snavely, R.A., Wilks, S.C., Town, R.P.J., Stephens, R., Campbell, E.M., Kodama, R., Mima, K., Tanaka, K.A., Atzeni, S. & Freeman, R. (2005). Review of progress in fast ignition. *Phys. Plasma* **12**, 057305.

Tabak, M., Hammer, J., Glinsky, M.E., Kruer, W.L., Wilks, S.C., Woodworth, J., Campbell, E.M. & Perry, M.D. (1994). Ignition and high gain with ultrapowerful lasers. *Phys. Plasma* **1**, 1626–1634.

Tommasini, R., Koch, J.A., Izumi, N., Welser, L.A., Mancini, R.C., Delettrez, J., Regan, S. & Smalyuk, V. (2006). Multispectral X-ray imaging for core temperature and density maps retrieval in direct drive implosions. *Rev. Sci. Instr*. **77**, 10E303.

Young, B.K.F., Osterheld, A.L., Price, D.F., Sheperd, R., Stewart, R.E., Faenov, A.Y., Magunov, A.I., Pikuz, T.A., Skobelev, I.Y., Flora, F., Bollanti, S., Lazzaro, P.D., Letardi, T., Grilli, A., Palladino, L., Reale, A., Scafati, A. & Reale, L. (1998). High-resolution X-ray spectrometer based on spherically bent crystals for investigations of femtosecond laser plasmas. *Rev. Sci. Instr*. **69**, 4049–4053.

Zamponi, F.A., Lübcke, A., Kämpfer, T., Uschmann, I., Förster, E., Giulietti, A., Giulietti, D., Köster, P., Labate, L., Levato, T. & Gizzi, L.A. (2009). Directional bremsstrahlung from a Ti laser-produced X-ray source at relativistic intensities in the 3–10 KeV range. *Phys. Rev. Lett*.

Zamponi, F., Kämpfer, T., Morak, A., Uschmann, I. & Förster, E. (2005). Characterization of a deep depletion, back-illuminated charge-coupled device in the X-ray range. *Rev. Sci. Instr*. **76**, 116101.

Zhong, J., Shiraga, H. & Azechi, H. (2008). One-dimensional and multichannels multi-imaging X-ray streak camera for imploded core plasma of shell-cone target. *Rev. Sci. Instr*. **79**, 10E907.